

MATTERS ARISING

<https://doi.org/10.1038/s41467-019-08704-1>

OPEN

# Reply to: “Thermal artefacts in two-photon solar cell experiments”

Shigeo Asahi<sup>1</sup> & Takashi Kita<sup>1</sup>

REPLYING TO C. C. Phillips *Nature Communications* <https://doi.org/10.1038/s41467-018-07166-1> (2019)

**T**wo-step photon up-conversion solar cells (TPU-SCs) are among the most promising photovoltaic devices<sup>1,2</sup>. In our previous works, we demonstrated the increase in the open-circuit voltage as well as the short-circuit current induced by the additional infrared (IR) light<sup>1</sup>. Phillips suggested that this phenomenon could be attributed to the sample heating<sup>2</sup>. Here, we present additional data suggesting that photoexcitation might be the cause. In the TPU-SC, the up-conversion is achieved by a series of two-step photoexcitation. By absorbing a below-gap photon, an electron transits from the valence band to the conduction band of the narrow bandgap semiconductor. Upon absorption of another below-gap photon, the electron accumulated at the hetero-interface is further pumped into the conduction band of the wide bandgap semiconductor. This ideal TPU process, following the absorption of two below-gap photons, produces additional photocurrent and boosts the photovoltage depending on the band offset at the hetero-interface. In this Reply to Matters Arising, we discuss the excitation power dependence of the external quantum efficiency (EQE) observed in TPU-SC and the efficient intraband excitation at the hetero-interface.

We measured the change in the EQE ( $\Delta$ EQE) of TPU-SCs with InAs quantum dots (QDs) as a function of interband excitation power density. Here,  $\Delta$ EQE was defined as the difference between the EQE obtained with and without the 1300 nm laser diode (LD) illumination. We conducted a systematic experiment to study the excitation power density dependence of the increased short-circuit current,  $\Delta J_{SC}$ , and the  $\Delta$ EQE. Detailed measurements taken at 300 K are presented in Fig. 1. We used a 784-nm continuous wave (CW) LD and a 1300-nm CW LD for the interband and the intraband excitations, respectively. With increasing interband excitation density, the  $\Delta J_{SC}$  increases sub-linearly and tends to deviate from the power law at high-excitation density above  $\sim 10 \text{ mW cm}^{-2}$ . Thereby,  $\Delta$ EQE significantly decreases with the interband excitation density. This set-up reproduces the results reported in our original article. Note that, in this experiment, we did not use a simulator and, indisputably, there were no artefacts of the simulator’s sensitive reference channel optical detectors with scattered laser light. Furthermore, we did not perform a signal modulation technique for the photocurrent

detection, because the lifetime of electrons separated from the holes can be extended to milliseconds<sup>3</sup>.

Here, we discuss the effects of thermal artefacts on the results. If  $\Delta J_{SC}$  is produced by the sample warming under the 1300-nm LD illumination,  $\Delta J_{SC}$  is given by

$$\Delta J_{SC} = J_{SC} \left[ \exp \left( -\frac{E_a}{k_b T + k_b \Delta T} + \frac{E_a}{k_b T} \right) - 1 \right], \quad (1)$$

where  $k_b$  is the Boltzmann constant,  $E_a$  is the activation energy,  $T$  is the temperature, and  $\Delta T$  is proportional to the 1300-nm LD power density. This gives an almost linear relationship in the measured region, as shown in Fig. 7b of the original article. However, the measured intraband excitation power density dependence in Fig. 7b was sublinear. Therefore,  $\Delta J_{SC}$  is not necessarily caused by thermal artefacts. We considered the possibility that the sublinear dependence of Fig. 7b arises from a change in the electron density at the hetero-interface. Figure 7d of the original article illustrates the dependence of the power-law index  $n$  on the reverse-bias voltage in the relationship of the intraband excitation power density and  $\Delta J$ . As the reverse-bias voltage increases,  $n$  increases and approaches unity. The space charge reduced by the intraband excitation weakens the electric field at the hetero-interface, resulting in a sub-linear response to the excitation density caused by the weaker electric field reducing the carrier collection efficiency of the TPU. We have recently reported the bias voltage dependence of  $n$  in detail (for example, ref. 4). The result is shown in Fig. 2, which reproduces the data of Fig. 7d of the original article. It is interesting to note that  $n$  quickly returns to unity by injecting carriers at the forward bias above  $\sim 0.4 \text{ V}$ . When enough carriers are injected, the influence of the accumulated electrons on the electric field near the hetero-interface is weakened. Thus, the sub-linear relationship between  $\Delta J$  and the interband excitation power density in Fig. 1 answers all questions. Accumulated electrons at the hetero-interface significantly influence the local electric field near the hetero-interface, which changes the carrier collection efficiency of the TPU. Therefore,  $\Delta J$  is determined by the number of intraband excited

<sup>1</sup> Department of Electrical and Electronic Engineering, Graduate School of Engineering, Kobe University, 1-1 Rokkodai, Nada, Kobe 657-8501, Japan. Correspondence and requests for materials should be addressed to S.A. (email: [asahis@people.kobe-u.ac.jp](mailto:asahis@people.kobe-u.ac.jp))

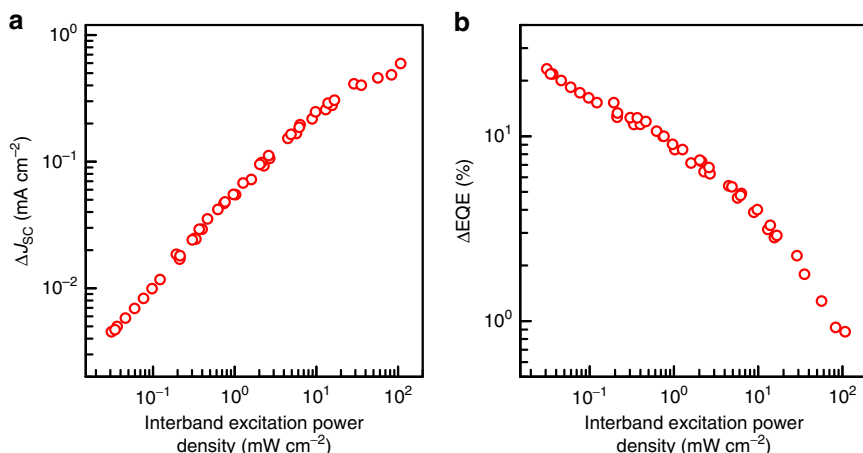


**Fig. 1** Interband excitation power density dependence of two-step photon up-conversion current at 300 K. **a** Change in the short-circuit current density ( $\Delta J_{sc}$ ). **b** Change in the external quantum efficiency ( $\Delta EQE$ ); the wavelength and excitation power density of the second intraband excitation light were 1300 nm and  $300 \text{ mW cm}^{-2}$ , respectively

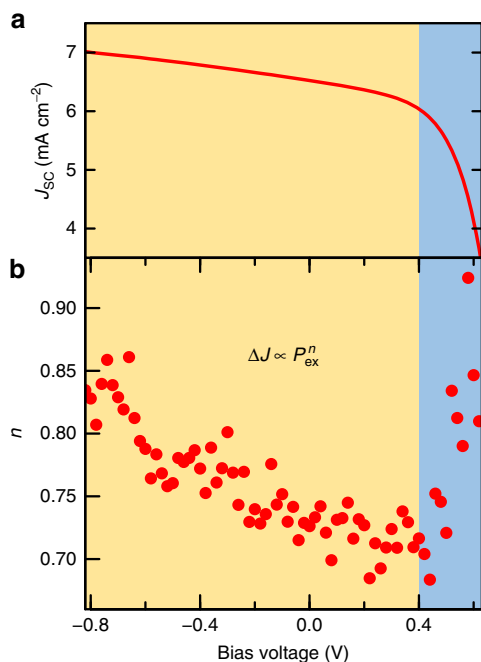


**Fig. 2** Bias voltage dependence of two-step photon up-conversion properties at 297 K. **a** Short-circuit current density ( $J_{sc}$ ). **b**  $n$  value of  $\Delta J_{sc} \propto P_{ex}^n$ , where  $\Delta J_{sc}$  is the change in the short-circuit current density, and  $P_{ex}$  is the 1300 nm excitation power density. The wavelength and excitation power density of the first interband excitation light were 780 nm and  $110 \text{ mW cm}^{-2}$ , respectively.  $P_{ex}$  was varied in the range  $1\text{--}320 \text{ mW cm}^{-2}$

carriers and their collection efficiency. Detailed analysis and the physics behind Fig. 1 will be discussed in our upcoming paper.

We next focus on the efficient intraband excitation occurring at the hetero-interface. Free carrier absorption should be considered at least in the TPU-SC without InAs QDs. If only the free carrier absorption occurs in the ‘bulk’ portion, the accumulated electron density becomes considerably high and causes a lower bound. It is well known that the wave-function of the accumulated electrons can generally penetrate the barrier layer. The wave-function penetration depth depends on the electric field at the hetero-interface. The penetrated component contributes to the transition from the confined level to the conduction band edge of AlGaAs,

which improves the excitation cross-section and, therefore, lowers the estimated electron sheet density. Such a mechanism can contribute to the improvement of the intraband excitation at the hetero-interface. Further experiments and theoretical work are necessary to unveil the efficient photoexcitation at the hetero-interface, which is the most important and interesting mechanism in TPU-SC.

The intermediate-band SC includes intermediate states in the bandgap. By absorbing a below-gap photon, an electron transits from the valence band to the intermediate band. Upon absorption of another below-gap photon, the electron is further excited into the conduction band. This ideal TPU process, following the absorption of two below-gap photons, produces additional photocurrent without degrading the photovoltage. However, it is well known that thermal coupling between the conduction band and the intermediate band gives rise to a reduction of  $V_{OC}$ . Many studies discussing the  $V_{OC}$  reduction have been published<sup>5</sup>. Similar processes occur at the hetero-interface of the TPU-SC. The photo-carrier generation of the TPU-SC without IR illumination indicates that the conduction bands of AlGaAs and GaAs are thermally coupled. The thermal coupling becomes stronger with rising temperature, which causes the change in  $V_{OC}$  according to Eq. (4) of the original article. This analytical model suggests that  $\Delta V_{OC}$  depends on the interband carrier density. We recently confirmed the strong dependence of the change in  $V_{OC}$  on the interband excitation density. The different trends, compared in Fig. 7e of the original article, are essential to demonstrate the contribution of the optical excitation process.

Finally, we would like to comment on the data error of the current–voltage ( $J$ – $V$ ) curve shown in Fig. 7a of the original article. The  $J$ – $V$  curve was drawn by smoothly connecting current density measured at discrete voltages at a step of every 0.02 V (see Fig. 3), and there is no real data point in the area magnified in the inset of the original Figure 7a. To better demonstrate the precision of  $J$ – $V$  curve and thus  $V_{OC}$  that can be extracted from our original measurements, we replot the magnification of  $J$ – $V$  curve around a zero current density in the inset of Fig. 3 here by highlighting the uncertainty induced by the errors in the original data. The shaded areas around the  $J$ – $V$  curve represent the standard error of the current density. It is clear that the uncertainty in our  $V_{OC}$  measurements is substantially smaller than the difference between  $V_{OC}$ s that can be extracted from the raw data at three irradiation conditions.

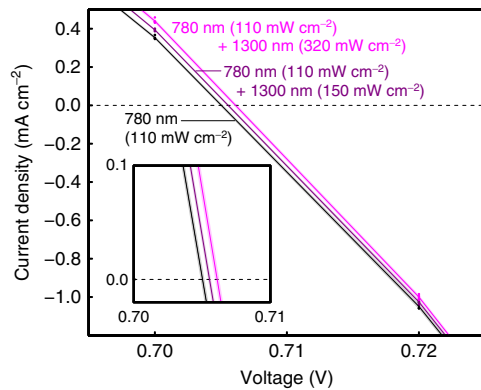


**Fig. 3** Current-voltage curve under the two-colour illumination of 780 nm and 1300 nm lasers: the solid circles indicate data points at 0.70 V and 0.72 V. The shaded areas represent the width of the standard error evaluated using the data. The inset shows the magnification of the open-circuit voltage curve as indicated in the inset of Fig. 7a of the original article. All data are the same as the data in the Fig. 7a, b, and c of the original article

### Data availability

The data that support the findings of this study are available from the corresponding author upon request.

Received: 20 July 2018 Accepted: 28 January 2019

Published online: 27 February 2019

### References

- Asahi, S., Teranishi, H., Kusaki, K., Kaizu, T. & Kita, T. Two-step photon up-conversion solar cells. *Nat. Commun.* **8**, 14962 (2017).
- Phillips, C. C. Thermal artefacts in two-photon solar cell experiments. *Nat. Commun.* <https://doi.org/10.1038/s41467-018-07166-1> (2019).
- Asahi, S. et al. Saturable two-step photocurrent generation in intermediate-band solar cells including InAs quantum dots embedded in Al<sub>0.3</sub>Ga<sub>0.7</sub>As/GaAs quantum wells. *IEEE J. Photovolt.* **6**, 465–472 (2016).

- Kusaki, K., Asahi, S., Kaizu, T. & Kita, T. Photon up-converted photocurrent in a single junction solar cell with a hetero-interface. In 34th European Photovoltaic Solar Energy Conference and Exhibition ICV.3.89. Amsterdam (2017).
- Okada, Y. et al. Intermediate band solar cells: recent progress and future directions. *Appl. Phys. Rev.* **2**, 021302 (2015).

### Acknowledgements

This work was partially supported by the Japan Society for the Promotion of Science (JSPS) KAKENHI Grant Number 18K18862 and 18KK0145.

### Author contributions

S.A. carried out experiments, performed modelling and data analysis, and wrote the manuscript. T.K. co-wrote the manuscript and was in charge of overall direction and planning.

### Additional information

**Competing interests:** The authors declare no competing interests.

**Reprints and permission** information is available online at <http://npg.nature.com/reprintsandpermissions/>

**Journal peer review information:** *Nature Communications* thanks the anonymous reviewers for their contribution to the peer review of this work.

**Publisher's note:** Springer Nature remains neutral with regard to jurisdictional claims in published maps and institutional affiliations.



**Open Access** This article is licensed under a Creative Commons Attribution 4.0 International License, which permits use, sharing, adaptation, distribution and reproduction in any medium or format, as long as you give appropriate credit to the original author(s) and the source, provide a link to the Creative Commons license, and indicate if changes were made. The images or other third party material in this article are included in the article's Creative Commons license, unless indicated otherwise in a credit line to the material. If material is not included in the article's Creative Commons license and your intended use is not permitted by statutory regulation or exceeds the permitted use, you will need to obtain permission directly from the copyright holder. To view a copy of this license, visit <http://creativecommons.org/licenses/by/4.0/>.

© The Author(s) 2019